

Metal-assisted coupling of oximes and nitriles: a synthetic, structural and theoretical study

Maxim L. Kuznetsov,^a Nadezhda A. Bokach,^b Vadim Yu. Kukushkin,^{*b} Tapani Pakkanen,^c Gabriele Wagner^a and Armando J. L. Pombeiro^{*a}

^a Centro de Química Estrutural, Complexo I, Instituto Superior Técnico, Av. Rovisco Pais, 1049-001 Lisbon, Portugal. E-mail: pombeiro@ist.utl.pt

^b Department of Chemistry, St. Petersburg State University, 198904 Stary Petergof, Russian Federation. E-mail: kukushkin@VK2100.spb.edu

^c Department of Chemistry, P.O. Box 111, FIN-80101, Joensuu, Finland. E-mail: Tapani.Pakkanen@joensuu.fi

Received 31st July 2000, Accepted 10th October 2000

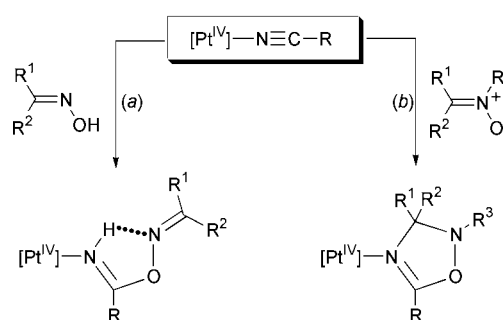
First published as an Advance Article on the web 23rd November 2000

Chlorination of $[\text{Ph}_3\text{PCH}_2\text{Ph}][\text{PtCl}_3(\text{EtCN})]$, obtained from the reaction of $[\text{PtCl}_2(\text{EtCN})_2]$ with $[\text{Ph}_3\text{PCH}_2\text{Ph}]\text{Cl}$, formed the platinum(IV) complex $[\text{Ph}_3\text{PCH}_2\text{Ph}][\text{PtCl}_5(\text{EtCN})]$ which, at ambient temperature and both in solution and in the solid phase, hydrolyses to the ammonia compound $[\text{Ph}_3\text{PCH}_2\text{Ph}][\text{PtCl}_5(\text{NH}_3)]$ and undergoes nucleophilic addition by ketoximes or amidoxime $\text{HON}=\text{CR}^1\text{R}^2$ [$\text{R}^1\text{R}^2 = \text{Me}_2, \text{C}_4\text{H}_8, \text{C}_5\text{H}_{10}, \text{C}_9\text{H}_{16}, \text{C}_9\text{H}_{18}$ or $\text{Ph}(\text{NH}_2)$] to give the corresponding iminoacylated product $[\text{Ph}_3\text{PCH}_2\text{Ph}][\text{PtCl}_5\{\text{HN}=\text{C}(\text{Et})\text{ON}=\text{CR}^1\text{R}^2\}]$. All compounds were characterized by elemental analyses, FAB mass spectrometry, IR and ^1H , ^{13}C - $\{^1\text{H}\}$, ^{31}P - $\{^1\text{H}\}$ and ^{195}Pt NMR spectroscopies. A crystal structure determination of $[\text{Ph}_3\text{PCH}_2\text{Ph}][\text{PtCl}_5\{\text{NH}=\text{C}(\text{Et})\text{ON}=\text{C}(\text{C}_9\text{H}_{16})\}]$ disclosed amidine one-end rather than the *N,N*-bidentate co-ordination mode of the *N*-donor ligand. The iminoacylation by oximes was investigated by *ab initio* methods (at RHF level using quasi-relativistic pseudopotentials for platinum) for $[\text{PtCl}_5(\text{NCMe})]^-$ which were also applied to the related neutral platinum(IV) $[\text{PtCl}_4(\text{NCMe})_2]$ and platinum(II) $[\text{PtCl}_2(\text{NCMe})_2]$ complexes. The calculations included geometry optimization of the starting and final complexes, location of possible transition states for the reaction discussed and intrinsic reaction coordinate calculations for one reaction. The results obtained provided an interpretation, on the basis of kinetic (activation energies) and thermodynamic (reaction energies) effects, for the order of reactivity observed [neutral $\text{Pt}^{\text{IV}} >$ anionic $\text{Pt}^{\text{IV}} >$ neutral Pt^{II}] and indicated that a mechanism based on nucleophilic addition of the protic nucleophile (undeprotonated oxime), to form a transition state with a four-membered NCOH ring, is energetically favoured relative to the alternative one involving prior deprotonation of the oxime, unless base-catalysed conditions are operating.

Introduction

The metal-assisted interaction between two organic molecules and/or ligands to give a larger and more complex molecular fragment is of basic scientific interest and also has potential industrial applications.¹ Being interested in the chemistry of both oximes²⁻⁴ and organonitriles,^{4,5} we have recently observed an unusual coupling between nitriles bound to the platinum(IV) center in $[\text{PtCl}_4(\text{RCN})_2]$ and oximes⁴ $\text{HON}=\text{CR}^1\text{R}^2$ or nitrones⁶ $^-\text{ON}^+(\text{R}^3)=\text{CR}^1\text{R}^2$ (the latter can be viewed as the “frozen”, by alkylation, form of the other oxime tautomer) to give the iminoacylated products $[\text{PtCl}_4(\text{HN}=\text{C}\{\text{R}\}\text{ON}=\text{CR}^1\text{R}^2)_2]$ due to the addition (Scheme 1(a))⁴ or Δ^4 -1,2,4-oxadiazoline compounds $[\text{PtCl}_4\{\text{N}=\text{C}(\text{Me})\text{ON}(\text{R}^3)\text{C}(\text{R}^1)(\text{R}^2)\}_2]$ as a result of [2 + 3] cycloaddition (Scheme 1(b)).⁶

Following many other works on the addition of different nucleophiles to metal-ligated RCN, *e.g.* amines, water, alcohols,⁷ mercaptans⁸ or phosphines,⁹ we have suggested that the addition of oximes (Scheme 1(a)) proceeds by nucleophilic attack of the oxime oxygen on the highly electrophilically activated carbon atom of the organonitrile. It was also anticipated that the latter property could be, in particular, reached by (i) application of metal ions in high and highest oxidation states, (ii) introducing acceptor groups R to RCN, (iii) increasing the overall positive charge on a complex ion and (iv) use of supporting ligands with pronounced π -acceptor properties. In accord with these hypotheses, we observed the facile additions of



Scheme 1 Reactions of Pt^{IV} -bound organonitriles with oximes and nitrones.

oximes to organonitrile species in complexes of $\text{Re}^{\text{IV}10}$ and $\text{Rh}^{\text{III}11}$ where the metal ions are in high oxidation states. Currently, it has been found that nitriles in complexes where the metal is in a relatively low oxidation state, *e.g.* the platinum(II) compounds $[\text{PtCl}_2(\text{RCN})_2]$ and $[\text{Pt}(\text{RCN})_2(\text{PPh}_3)_2][\text{BF}_4]_2$ ($\text{R} = \text{CH}_2\text{Ph}, \text{NMe}_2$ or NEt_2),¹² do not undergo the addition of the oximes (Scheme 1(a)) in spite of, in the latter case, the significant overall positive charge on the complex ion and the availability of the co-ordinated phosphines possessing π -acceptor properties. However, oximes can be added to the complexes with dialkylcyanamides $[\text{Pt}(\text{RCN})_2(\text{PPh}_3)_2]^{2+}$ ($\text{R} = \text{NMe}_2$ or NEt_2) in the presence of Lewis acids such as Ag^+ or Cu^{2+} which

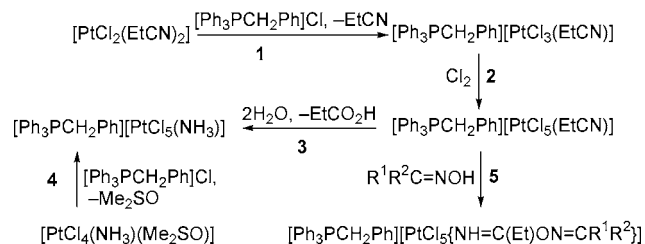
metallate the dialkylamido group thus providing additional activation of the nitrile group.¹²

As a part of our investigations we have now studied the addition of ketoximes and benzamide oxime to the anionic platinum(IV) compound $[\text{PtCl}_5(\text{EtCN})]^-$. Our interest in extension of our previous work on neutral complexes⁴ to this complex was, at least, twofold. First, we attempted to understand factors affecting the coupling of nitriles and oximes and, in particular, to verify the role of the overall negative charge on the addition of oximes. Second, we intended to show whether the addition is restricted only to neutral compounds or has a more general character. In contrast to our expectations, we found that the oximes can be added rather readily to the ethyl cyanide ligand thus indicating the absence of any significant effect of the negative charge on the addition. In order to answer the question "why the addition was not detected in the case of the platinum(II) compounds $[\text{PtCl}_2(\text{RCN})_2]$, while it is facile in the cases of both neutral and anionic platinum(IV) complexes $[\text{PtCl}_4(\text{RCN})_2]$ and $[\text{PtCl}_5(\text{EtCN})]^-$ ", a theoretical study has been carried out and its results along with synthetic and structural data on the addition products $[\text{Ph}_3\text{PCH}_2\text{Ph}][\text{PtCl}_5\{\text{HN}=\text{C}(\text{Et})\text{ON}=\text{CR}^1\text{R}^2\}]$ [$\text{R}^1\text{R}^2 = \text{Me}_2, \text{C}_4\text{H}_8, \text{C}_5\text{H}_{10}, \text{C}_9\text{H}_{16}, \text{C}_9\text{H}_{18}$ or $\text{Ph}(\text{NH}_2)$] are reported in this article.

Results and discussion

Synthesis and hydrolysis of the starting nitrile complexes

For this study we addressed the platinum(IV) complex $[\text{Ph}_3\text{PCH}_2\text{Ph}][\text{PtCl}_5(\text{EtCN})]$ with the highly lipophilic cation and Et radical at the nitrile group which provide good solubility in the most common organic solvents. The precursor for the preparation of $[\text{Ph}_3\text{PCH}_2\text{Ph}][\text{PtCl}_5(\text{EtCN})]$, *i.e.* the appropriate platinum(II) complex $[\text{Ph}_3\text{PCH}_2\text{Ph}][\text{PtCl}_3(\text{EtCN})]$, was obtained in the course of the reaction between $[\text{PtCl}_2(\text{EtCN})_2]$ and $[\text{Ph}_3\text{PCH}_2\text{Ph}]\text{Cl}$ in chloroform (reaction 1, Scheme 2). The



Scheme 2 Synthetic routes.

latter method gives a pure product in high yield and certainly has advantages over alternative procedures for the synthesis of $[\text{Cation}][\text{PtCl}_3(\text{RCN})]$ complexes¹³ which are either time-consuming or result in a low yield of the product. Chlorination of $[\text{Ph}_3\text{PCH}_2\text{Ph}][\text{PtCl}_3(\text{EtCN})]$ by Cl_2 in CHCl_3 afforded $[\text{Ph}_3\text{PCH}_2\text{Ph}][\text{PtCl}_5(\text{EtCN})]$ (reaction 2, Scheme 2).

The platinum(II) and platinum(IV) complexes $[\text{Ph}_3\text{PCH}_2\text{Ph}][\text{PtCl}_3(\text{EtCN})]$ and $[\text{Ph}_3\text{PCH}_2\text{Ph}][\text{PtCl}_5(\text{EtCN})]$ give very similar ^1H , ^{13}C - $\{^1\text{H}\}$ and ^{31}P - $\{^1\text{H}\}$ NMR spectra but can easily be distinguished by ^{195}Pt NMR ($\delta -2021$ vs. -184 , correspondingly). The platinum(IV) complex $[\text{Ph}_3\text{PCH}_2\text{Ph}][\text{PtCl}_5(\text{EtCN})]$ is stable in a vacuum desiccator over KOH but gradually decomposed in open air. Column chromatography of the products of decomposition allowed the separation of the ammonia compound $[\text{Ph}_3\text{PCH}_2\text{Ph}][\text{PtCl}_5(\text{NH}_3)]$ (reaction 3, Scheme 2). The latter was also obtained by independent synthesis¹⁴ on treatment of $[\text{PtCl}_4(\text{NH}_3)(\text{Me}_2\text{SO})]$ with $[\text{Ph}_3\text{PCH}_2\text{Ph}]\text{Cl}$ in chloroform (reaction 4, Scheme 2) and the authenticity of the two samples was confirmed by comparison of their characteristics listed in the Experimental section. The same ammonia complex, along with some other species which were not separated and identified, was observed on maintaining $[\text{Ph}_3\text{PCH}_2\text{Ph}][\text{PtCl}_5(\text{EtCN})]$ in a non-dried chloroform solution. The hydrolytic degradation is slow and a rather significant amount of $[\text{Ph}_3\text{PCH}_2\text{Ph}][\text{PtCl}_5(\text{NH}_3)]$ is detected only after 2 d at 20–25 °C in the solution or after 5 d in the solid phase in the open air. The conversion of EtCN is obviously metal-mediated since hydrolysis of organonitriles RCN with electron-donor groups R requires harsh reaction conditions.¹⁵ It should be pointed out that the two-step metal-mediated hydrolysis of co-ordinated organonitriles to give ammonia-containing products is still a rare phenomenon and it was previously reported only for platinum(IV)¹⁶ and niobium(V) systems,¹⁷ while in other documented cases the hydrolysis of metal-bound nitriles gave carboxamides or tautomeric iminols depending on the nature of metal centre.^{7,18}

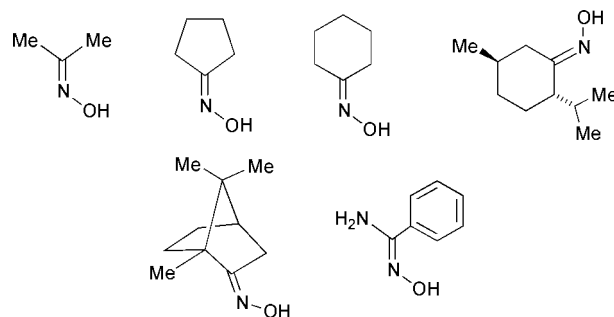


Fig. 1 Oximes used for the coupling.

It is worthwhile to mention that ^1H and ^{195}Pt NMR spectra of the anion $[\text{PtCl}_5(\text{NH}_3)]^-$ exhibit an interesting coupling pattern due to an exceptionally slow relaxation of the ^{14}N nuclei of the NH_3 ligand in $\text{DMSO}-d_6$ solution. Thus, the ^1H signal of the co-ordinated NH_3 appears as three lines of equal intensity due to a well resolved coupling to ^{14}N ($J_{\text{H}^{14}\text{N}}$ 53 Hz) and each of these lines showing ^{195}Pt satellites with J_{PtH} 52 Hz. In the ^{195}Pt NMR spectrum the same J_{PtH} can be observed as a quartet fine structure of the three line spectrum caused by coupling of ^{195}Pt to ^{14}N ($J_{\text{H}^{14}\text{N}}$ 169 Hz). Such cases of resolved ^{14}N coupling are described for cyanate, thiocyanate and isocyanide complexes of Pt,¹⁹ but, to our knowledge, have never been observed in $\text{Pt}(\text{NH}_3)$ or $\text{Pt}(\text{amine})$ complexes.

It is worthwhile to mention that ^1H and ^{195}Pt NMR spectra of the anion $[\text{PtCl}_5(\text{NH}_3)]^-$ exhibit an interesting coupling pattern due to an exceptionally slow relaxation of the ^{14}N nuclei of the NH_3 ligand in $\text{DMSO}-d_6$ solution. Thus, the ^1H signal of the co-ordinated NH_3 appears as three lines of equal intensity due to a well resolved coupling to ^{14}N ($J_{\text{H}^{14}\text{N}}$ 53 Hz) and each of these lines showing ^{195}Pt satellites with J_{PtH} 52 Hz. In the ^{195}Pt NMR spectrum the same J_{PtH} can be observed as a quartet fine structure of the three line spectrum caused by coupling of ^{195}Pt to ^{14}N ($J_{\text{H}^{14}\text{N}}$ 169 Hz). Such cases of resolved ^{14}N coupling are described for cyanate, thiocyanate and isocyanide complexes of Pt,¹⁹ but, to our knowledge, have never been observed in $\text{Pt}(\text{NH}_3)$ or $\text{Pt}(\text{amine})$ complexes.

Coupling reaction and characterization of products

The anionic complex in $[\text{Ph}_3\text{PCH}_2\text{Ph}][\text{PtCl}_5(\text{EtCN})]$ reacts with one equivalent of the oxime $\text{HON}=\text{CR}^1\text{R}^2$ [$\text{R}^1\text{R}^2 = \text{Me}_2, (\text{CH}_2)_4, (\text{CH}_2)_5, \text{C}_9\text{H}_{18}, \text{C}_9\text{H}_{16}$ or $(\text{NH}_2)\text{Ph}$] (structures of the oximes are depicted in Fig. 1) under mild conditions to afford (80–90% yield) the addition products $[\text{Ph}_3\text{PCH}_2\text{Ph}][\text{PtCl}_5\{\text{NH}=\text{C}(\text{Et})\text{ON}=\text{CR}^1\text{R}^2\}]$ (reaction 5, Scheme 2). The IR spectra of the products do not show any bands due to $\nu(\text{C}\equiv\text{N})$ stretching vibrations but display very strong $\nu(\text{C}=\text{N})$ bands [$1630\text{--}1656\text{ cm}^{-1}$] and rather weak bands in the range $3277\text{--}3299\text{ cm}^{-1}$ which were attributed to $\nu(\text{N}\text{--}\text{H})$ stretching vibrations. Attribution of medium-intensity $\nu(\text{C}\text{--}\text{O})$ vibrations is unreliable due to overlapping with strong bands of the phosphonium counter ion. FAB⁻ spectra display the molecular peak of an anionic platinum complex, accompanied by a typical fragmentation pattern to give $[\text{PtCl}_5]^-$, $[\text{PtCl}_4]^-$, $[\text{PtCl}_3]^-$ and $[\text{PtCl}_2]^-$ fragment ions. In ^1H and ^{13}C - $\{^1\text{H}\}$ NMR spectra the signals due to the $\text{HN}=\text{C}$ moiety are in the same range as observed for analogous neutral complexes.⁴ ^{195}Pt NMR spectra turned out to be the most sensitive method to distinguish between the neutral compounds $[\text{PtCl}_4\{\text{NH}=\text{C}(\text{R})\text{ON}=\text{CR}^1\text{R}^2\}]$ and the anionic $[\text{PtCl}_5\{\text{NH}=\text{C}(\text{R})\text{ON}=\text{CR}^1\text{R}^2\}]^-$. Indeed, the chemical shifts of the anionic complexes ($\delta +20$ to -2) are closer to that of $[\text{PtCl}_6]^{2-}$ ion ($\delta 0$) than of the corresponding neutral complexes ($\delta -155$ to -160). All applied NMR methods show only signals corresponding to one isomerically pure compound and no evidence for the existence of mixtures of *E/Z* isomers in solution was obtained. All these observed spectroscopic data are in good

Table 1 Bond lengths (Å) and angles (°) for one of two crystallographically independent anions in $[\text{Ph}_3\text{PCH}_2\text{Ph}][\text{PtCl}_5\{\text{NH}=\text{C}(\text{Et})\text{ON}=\text{C}(\text{C}_9\text{H}_{16})\}]$

Pt(1)–Cl(1)	2.322(7)	C(4)–C(5)	1.53(5)
Pt(1)–Cl(2)	2.316(7)	C(5)–C(6)	1.56(6)
Pt(1)–Cl(3)	2.313(7)	C(6)–C(7)	1.38(6)
Pt(1)–Cl(4)	2.293(6)	C(7)–C(8)	1.64(6)
Pt(1)–Cl(5)	2.302(8)	C(8)–C(9)	1.42(4)
Pt(1)–N(1)	1.943(17)	C(9)–C(4)	1.40(4)
N(1)–C(1)	1.31(4)	C(9)–C(13)	1.62(5)
C(1)–C(2)	1.43(5)	C(9)–C(10)	1.47(5)
C(2)–C(3)	1.30(7)	C(6)–C(10)	1.58(5)
C(1)–O(1)	1.40(4)	C(10)–C(11)	1.51(5)
O(1)–N(2)	1.38(3)	C(10)–C(12)	1.61(6)
N(2)–C(4)	1.26(3)		
Cl(4)–Pt(1)–N(1)	173.3(5)	N(2)–C(4)–C(9)	128(3)
Cl(5)–Pt(1)–N(1)	95.0(5)	C(1)–C(2)–C(3)	121(4)
Cl(1)–Pt(1)–Cl(2)	177.7(2)	C(4)–C(5)–C(6)	102(3)
Cl(1)–Pt(1)–Cl(3)	91.3(2)	C(5)–C(6)–C(7)	98(3)
Cl(1)–Pt(1)–Cl(4)	92.0(2)	C(6)–C(7)–C(8)	113(3)
Cl(1)–Pt(1)–Cl(5)	88.3(3)	C(7)–C(8)–C(9)	93(3)
Cl(1)–Pt(1)–N(1)	83.3(5)	C(4)–C(9)–C(8)	107(2)
Cl(2)–Pt(1)–Cl(3)	89.4(2)	C(5)–C(4)–C(9)	108(3)
Cl(2)–Pt(1)–Cl(4)	90.2(2)	C(8)–C(9)–C(10)	103(3)
Cl(2)–Pt(1)–Cl(5)	91.0(3)	C(7)–C(6)–C(10)	93(3)
Cl(2)–Pt(1)–N(1)	94.6(6)	C(5)–C(6)–C(10)	102(3)
Cl(3)–Pt(1)–Cl(4)	91.0(2)	C(4)–C(9)–C(10)	107(2)
Cl(3)–Pt(1)–Cl(5)	179.3(2)	C(8)–C(9)–C(13)	116(3)
Cl(3)–Pt(1)–N(1)	84.4(5)	C(4)–C(9)–C(13)	113(3)
Cl(4)–Pt(1)–Cl(5)	89.5(3)	C(10)–C(9)–C(13)	109(3)
Pt(1)–N(1)–C(1)	139.5(17)	C(6)–C(10)–C(12)	93(3)
N(1)–C(1)–C(2)	124(3)	C(11)–C(10)–C(12)	105(3)
O(1)–C(1)–N(1)	121(2)	C(6)–C(10)–C(9)	97(2)
N(2)–O(1)–C(1)	113(2)	C(6)–C(10)–C(11)	118(3)
O(1)–N(2)–C(4)	114(2)	C(9)–C(10)–C(11)	116(3)
O(1)–C(1)–C(2)	115(3)	C(9)–C(10)–C(12)	108(3)
N(2)–C(4)–C(5)	123(3)		

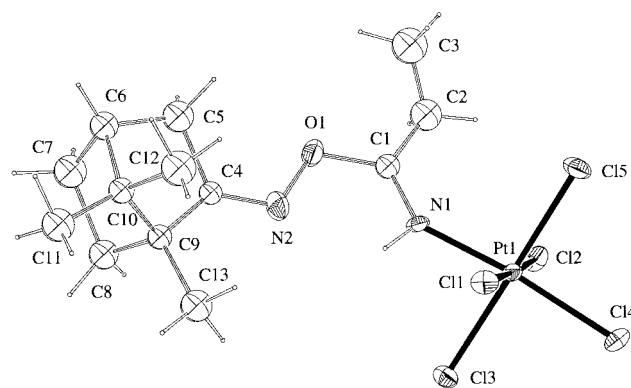


Fig. 2 View of the anion in $[\text{Ph}_3\text{PCH}_2\text{Ph}][\text{PtCl}_5\{\text{NH}=\text{C}(\text{Et})\text{ON}=\text{C}(\text{C}_9\text{H}_{16})\}]$ with the atomic numbering scheme.

agreement with those found⁴ in cases of $[\text{PtCl}_4\{\text{NH}=\text{C}(\text{R})\text{ON}=\text{CR}^1\text{R}^2\}_2]$ complexes.

The structure of $[\text{Ph}_3\text{PCH}_2\text{Ph}][\text{PtCl}_5\{\text{NH}=\text{C}(\text{Et})\text{ON}=\text{C}(\text{C}_9\text{H}_{16})\}]$ was determined by X-ray single-crystal diffraction (Fig. 2, Table 1). The compound crystallizes in a non-centrosymmetric space group ($P2_1$) due to the chirality present in the camphor moiety of the oxime. The unit cell contains two pairs of both anionic complex and counter ion whose bond lengths and angles have normal values.^{4,20} The ligand adopts an *E* conformation which is held by a hydrogen bond between the imino NH and the oxime nitrogen [N(1)⋯N(2), N(1)–H, N(1)H⋯N(2) are 2.61, 0.9132 and 2.1233 Å, N(1)–H⋯N(2) is 112.448°].

In spite of the negative charge of the starting platinum complex with five strong electron-releasing Cl^- ligands and of the electron-donor character of the alkyl group of the ligated EtCN, the latter ligand is readily activated towards addition of

a mild nucleophile, an oxime, and this somehow unpredictable behaviour was subject to a theoretical investigation which is described below.

Theoretical study

Our general intention was to verify the role of ligation of nitriles to metal centers in their reactivity towards nucleophilic addition of oximes and to study the effect of oxidation state and overall charges of the complex moieties on the organonitrile reactivity. In particular, we attempted to answer the question why the addition was not detected in platinum(II) complexes, while it is facile in both neutral and anionic complexes of platinum(IV). The main steps undertaken to clarify these features include: (i) the full geometry optimization of the platinum acetonitrile complexes *trans*- $[\text{PtCl}_2(\text{MeCN})_2]$ **1**, $[\text{PtCl}_5(\text{MeCN})]^-$ **2** and *trans*- $[\text{PtCl}_4(\text{MeCN})_2]$ **3** (Fig. 3) and analysis of factors which, in principle, can determine the reactivity of nitriles, e.g. effective atomic charges, energy and composition of the frontier molecular orbitals (systems **1–3** with different metal oxidation states and overall charges on the complexes were chosen for this work); (ii) determination of the energetic features of the discussed reaction with an oxime ($\text{HON}=\text{CH}_2$) and the study of plausible mechanisms including full geometry optimization of final products of the addition, location of the transition states for these reactions, intrinsic reaction coordinate calculations and estimate of the activation and reaction energies.

Equilibrium structures of complexes 1–3. Theoretically calculated selected bond lengths for the acetonitrile complexes **1–3** are given in Table 2. The co-ordination polyhedra are square planar (**1**) and octahedral (**2**, **3**) with linear acetonitrile ligands. The Pt–Cl bond lengths [equatorial ones for **2**] slightly decrease from **1** to **3**. In **2** the axial bond is 0.070 Å shorter than the equatorial ones. In **1** and **3**, the Pt–N bonds are equivalent within each complex and the longest bond is observed for **2**. The C≡N and C–C bond lengths are very similar, within 0.003 Å, for all three complexes. The calculated Pt–Cl and Pt–N bond lengths are somewhat longer (by 0.074–0.075 and 0.081 Å) than those observed experimentally for **1**.²¹

Inspection of the calculated Mulliken atomic charges on the nitrile carbon in free CH_3CN [0.12] (geometry optimization at 6-31 G basis set) and in the platinum complexes **1** [0.18], **2** [0.15], and **3** [0.19] indicates that (i) the positive charge on the nitrile C atom only slightly increases upon co-ordination, (ii) the charges on the carbon are similar for all three complexes and it appears that neither the oxidation state of the Pt nor the overall negative charge on **2** affects significantly these values.

In terms of the frontier orbital theory²² it is generally believed that nucleophilic additions to a substrate are mostly determined by the composition of its LUMOs. The analysis of the molecular orbital composition (the HOMO and LUMO of **2** are given in Fig. 4) shows that the HOMOs of complexes **2** and **3** are centred on the Cl atoms, while in **1** the contributions of orbitals of both Cl and Pt atoms are significant. The orbitals of the acetonitrile ligand do not participate in the HOMOs, consistent with the weak π -acceptor properties of MeCN. The LUMO of **3** consists of d orbitals of the Pt atom, which interact antibondingly with the appropriate p orbitals of the Cl atoms and without any contribution from the MeCN orbitals. The LUMO of **1** and **2** is formed by s and d orbitals of Pt with some contribution of s orbitals of N and C atoms. All the above results show that the absence of remarkable reactivity of **1** towards nucleophilic addition of oximes and the significant reactivity of both **2** and **3** cannot clearly be rationalized on the basis of effective atomic charge considerations (insignificant difference in charges on the nitrile C atom for **1–3**) and analysis of composition of frontier molecular orbitals (absence or low contribution of MeCN orbitals in the LUMOs of **2** and **3**).

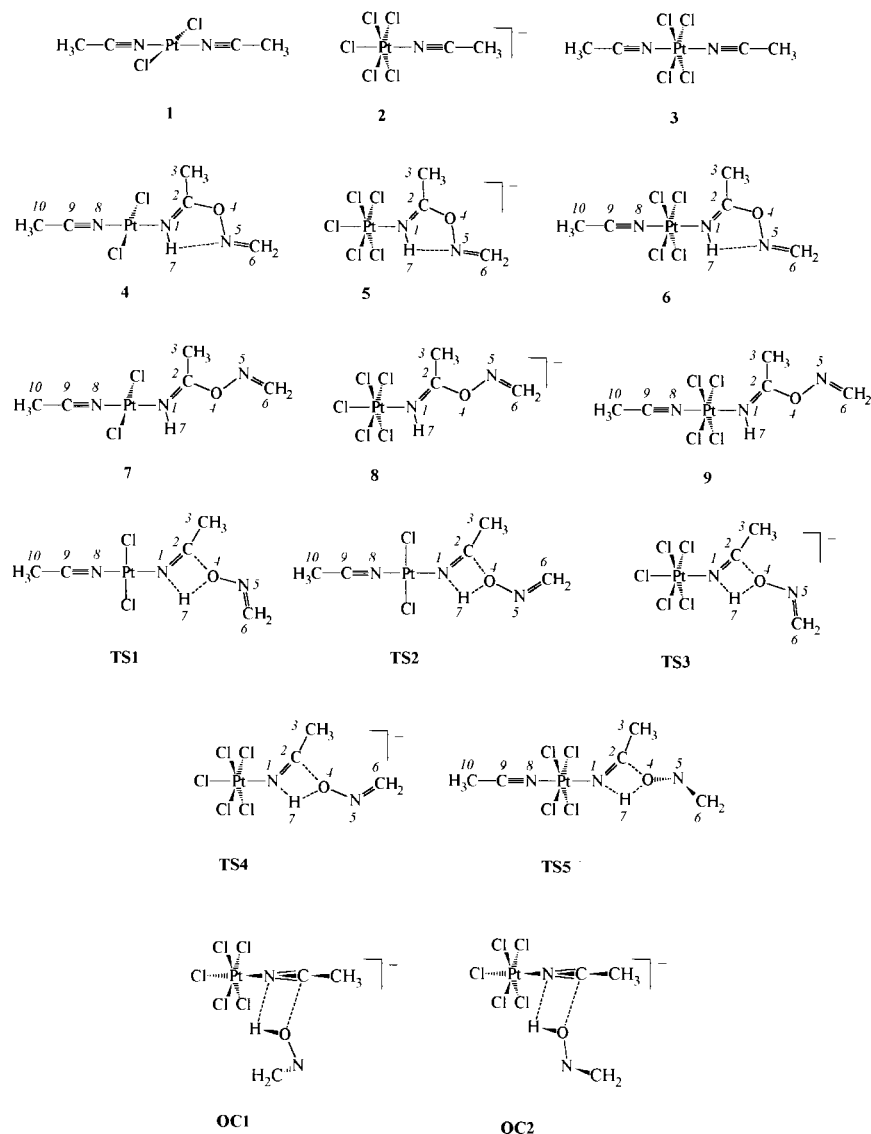


Fig. 3 The starting complexes (1–3), products of the addition (4–9) and structures of transition states (TS1–TS5) and the orientation complexes (OC1, OC2) with numbering of selected atoms.

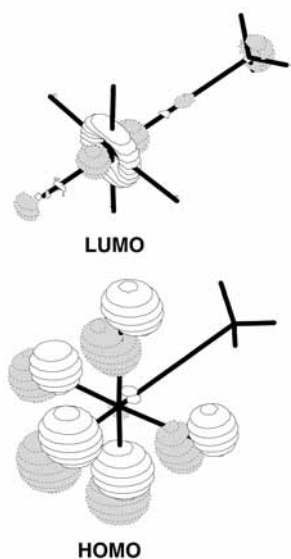


Fig. 4 Plots of the HOMO and LUMO for complex 2.

Similar results were obtained using the other basis sets, *i.e.* 3-21G, 6-31G*, DH for non-Pt atoms and the same basis set and ECP (effective core potential) for Pt, as well as the electron

correlation correction (for 2, MP2//MP2// approach), showing low sensitivity of the calculated *relative* values of atomic charges, although the *absolute* values are significantly different, and of the composition of the frontier MOs of 1–3 on change of the basis set.

Equilibrium structures of the addition products. A search for the equilibrium geometries of possible products of the addition of formaldoxime to complexes 1–3, *i.e.* *trans*-[PtCl₂(MeCN){NH=C(Me)ON=CH₂}], [PtCl₅{NH=C(Me)ON=CH₂}][−] and *trans*-[PtCl₄(MeCN){NH=C(Me)ON=CH₂}₂], was carried out and, as a result, two structures, which differ in the conformation of the oxime fragment, were located for each complex. The structures 4–6 (Fig. 3) are more stable than 7–9 (by 0.11, 0.10 and 0.11 eV, correspondingly) and, in accord with the calculations, conformations similar to 4–6 were observed experimentally for *trans*-[PtCl₄{NH=C(R)ON=CR¹R²}]₂^{4,23} and [Ph₃PCH₂Ph][PtCl₅{NH=C(Et)ON=CR¹R²}] (see above). These conformations are stabilized by the intramolecular hydrogen bond N(1)–H(7)···N(5) with the following parameters: N(1)···N(5), N(1)–H and N(1)H···N(5) are 2.67, 1.00 and 2.24 Å for 4, 2.67, 1.00 and 2.23 Å for 5, 2.64, 1.00 and 2.18 Å for 6 and with the angle N–H···N 104.7, 104.9 and 106.4° for 4, 5 and 6, respectively. The calculated N–H lengths are longer than the experimental ones, since they are underestimated in X-ray diffraction analysis.²⁴

Table 2 Theoretically calculated selected bond lengths (Å) for the starting complexes (1–3), the products of addition of undepronated formaldoxime (4–9), depronated formaldoxime (10–15) and the transition states (TS1–TS5)

	1	2	3
Pt–Cl	2.370; 2.371	eq. 2.367 (ax. 2.297)	2.356
Pt–N	2.025	2.070	1.994
C≡N	1.135	1.133	1.132
C–C	1.458	1.456	1.458
	4	5	6
Pt–Cl	2.373; 2.382	eq. 2.366–2.372 (ax. 2.322)	2.354–2.362
Pt–N(1)	2.046	2.084	2.016
C(2)N(1)	1.264	1.260	1.271
C(2)C(3)	1.487	1.486	1.487
CO	1.363	1.377	1.356
ON	1.425	1.416	1.430
	7	8	9
Pt–Cl	2.374; 2.381	eq. 2.367–2.370 (ax. 2.321)	2.355–2.361
Pt–N(1)	2.046	2.082	2.014
C(2)N(1)	1.267	1.262	1.274
C(2)C(3)	1.488	1.486	1.486
CO	1.362	1.376	1.354
ON	1.425	1.414	1.430
	10	11	12
Pt–Cl	2.411, 2.414	2.411, 2.412	eq. 2.380–2.384 (ax. 2.426)
Pt–N(1)	1.999	2.000	2.015
C(2)N(1)	1.231	1.232	1.236
C(2)C(3)	1.503	1.504	1.501
CO	1.442	1.453	1.441
ON	1.394	1.392	1.396
	13	14	15
Pt–Cl	eq. 2.372–2.391 (ax. 2.424)	2.363–2.377	2.364–2.379
Pt–N(1)	2.024	1.973	1.980
C(2)N(1)	1.231	1.243	1.243
C(2)C(3)	1.497	1.497	1.498
CO	1.473	1.421	1.430
ON	1.393	1.421	1.394
	TS1	TS2	TS3
Pt–Cl	2.373; 2.384	2.362; 2.388	eq. 2.355–2.379 (ax. 2.299)
Pt–N(1)	2.035	2.053	2.103
C(2)N(1)	1.204	1.199	1.186
C(2)C(3)	1.466	1.464	1.453
CO	1.706	1.804	1.916
ON	1.395	1.382	1.373
N(1)H(7)	1.400	1.292	1.265
O(4)H(7)	1.208	1.275	1.294
	TS4	TS5	
Pt–Cl	eq. 2.348–2.385 (ax. 2.295)	2.352–2.365	
Pt–N(1)	2.123	1.986	
C(2)N(1)	1.187	1.228	
C(2)C(3)	1.454	1.472	
CO	1.957	1.540	
ON	1.367	1.436	
N(1)H(7)	1.221	1.478	
O(4)H(7)	1.336	1.162	

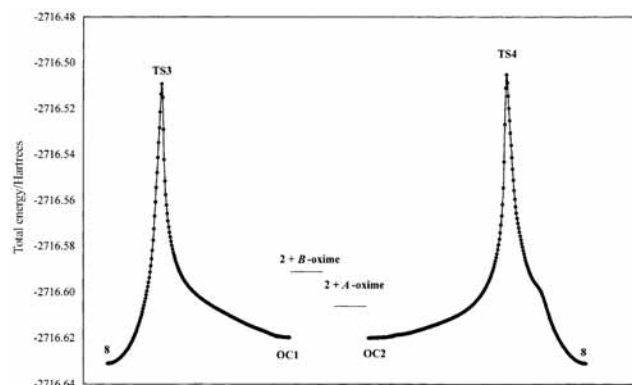


Fig. 5 Calculated intrinsic reaction coordinate using the transition states **TS3** and **TS4** as starting points.

The bond lengths of the different conformations of *trans*-[PtCl₂(MeCN){NH=C(Me)ON=CH₂}], [PtCl₅{NH=C(Me)ON=CH₂}][−] and *trans*-[PtCl₄(MeCN){NH=C(Me)ON=CH₂}₂] are almost the same for each particular complex and the structural parameters of the NH=C(Me)ON=CH₂ fragment in **5** and **6** (Table 2) are in good agreement with a rather large amount of experimental X-ray structural data for the complexes of the type *trans*-[PtCl₄{NH=C(R)ON=CR¹R²}₂]^{4,23} as well as for [Ph₃PCH₂Ph][PtCl₅{NH=C(Et)ON=CR¹R²}] (see above). The maximum difference between the calculated and average experimental bond lengths is observed for Pt–Cl and Pt–N bonds (except the Pt–N(1) bond in **6**) but it does not exceed 0.10 Å. The deviations for other bond lengths are not higher than 0.02 (for **6**) or 0.03 Å (for **5**) and the latter value is smaller than the e.s.d.s for [Ph₃PCH₂Ph][PtCl₅{NH=C(Et)ON=CR¹R²}].

Transition states and reaction paths. Although the kinetics and mechanisms of the reaction of metal-bound organonitriles and some nucleophiles such as amines or alcohols have been investigated only in a limited number of cases, all authors⁷ believe that the reaction takes place *via* approach of the coordinated organonitrile by an undepronated nucleophile to form a four-membered transition state (TS) followed by its rearrangement to give amidines or amido esters, correspondingly. In accord with this viewpoint, attempts to find saddle points corresponding to transition states for the discussed reaction were undertaken. Two (**TS1**, **TS2** and **TS3**, **TS4**) transition states were located for the reactions of formaldoxime with complexes **1** and **2**, respectively, but only one (**TS5**) was found in the case of **3**. For all transition states the hydrogen atom H(7) is localized between the N(1) and O(4) atoms with N(1)⋯H(7) and O(4)⋯H(7) distances of 1.221–1.478 and 1.162–1.336 Å and NHO angles of 103.8–116.9° (Table 2). The C⋯O distances are in the range 1.540–1.957 Å, the C(2)N(1) bond length increases as compared to those of **1–3** but remains shorter than those for the final complexes **4–9**, corresponding to a decrease in the CN bond orders from **1–3** to TS and further to **4–9**.

Calculations of the intrinsic reaction coordinate (IRC) starting from both **TS3** and **TS4** were carried out for the anionic species (Fig. 5) and the results obtained suggest that the addition of formaldoxime to complex **2** can proceed in two ways. The first route (*a* in Scheme 3) starts from a change of the oxime conformation from the more stable *A* to the less stable (by 0.38 eV) *B*. Then the approach of **2** by the oxime leads to orientation complex (**OC1**, Fig. 3) with N⋯H and O⋯C distances of *ca.* 3 Å whose energy is 0.76 and 0.37 eV lower than that of **2** plus of *B*- or *A*-oxime, respectively. Transformation of **OC1** with further approach between **2** and the oxime is accompanied by bending of the PtNCC and NCC fragments that leads to polarization of the CN and OH bonds (increase of the

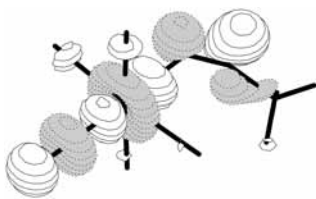
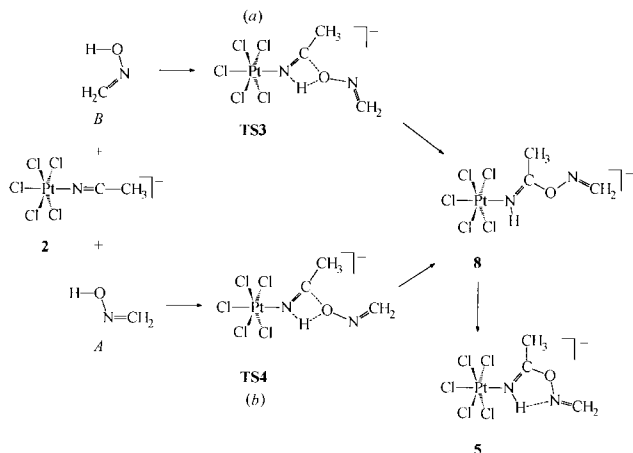


Fig. 6 Plot of the LUMO for complex 2'.



Scheme 3 Representation of the mechanism of addition to complex 2.

absolute values of effective atomic charges on the corresponding atoms) and correlates with the change in hybridization of the nitrile group C and N atoms and promotes nucleophilic addition to acetonitrile. Finally, the formation of short contacts $N \cdots H$ and $C \cdots O$ is concerted with weakening of the oxime O–H bond and subsequent bending of the PtNC and NCC fragments is observed giving the transition state **TS3**. On the way from **TS3** to the final complex, formation of N–H and C–O bonds accompanying OH bond cleavage takes place and the structure **8** is formed.

The bending of the acetonitrile site which takes place during the reaction leads to a decrease of the LUMO energy of complex **2** and to a change of its composition. Thus, the formation of the CO and NH bonds in the last steps of the reaction can be rationalized in terms of frontier molecular orbital theory. Indeed, as was noticed above, the contribution of orbitals of the MeCN ligand in the LUMO of **2** is rather small. Single-point calculations of the starting complex **2** but with bending acetonitriles (**2'**) (formed on the basis of **TS3** by removing the ONCH₂ oxime fragment and H(7) atom) indicate that the orbitals of the nitrile group C and N atoms give significant contributions to the LUMO of this structure (besides the orbitals of Pt and Cl, Fig. 6). Furthermore, the energy of the LUMO decreases relatively to that of **2**. Such changes in the composition and energy of the LUMO facilitate nucleophilic addition to the co-ordinated acetonitrile and determine the formation of the final complex.

Another route (*b* in Scheme 3) is initiated by the approach to complex **2** by the oxime molecule in the *A* conformation followed by formation of the orientation complex **OC2** with $N \cdots H$ and $O \cdots C$ distances of 3.03 and 3.14 Å, correspondingly, whose energy is 0.38 eV lower than that of **2** plus *A*-oxime, with further transformation to the **TS4** (Fig. 5). It is worthwhile to note that IRC calculations on the route from **TS4** to the addition product show that the formation of **5** directly from **TS4** does not occur, although it should be accompanied by minor structural changes. Instead, **8** is formed followed by its conversion into **5** and the latter structure agrees well with the experimentally observed conformation of the iminoacyl ligand. Concerning the coupling reaction starting from **3**, we were unable to locate the TS, similar to **TS4**, although that analo-

gous to **TS3** (*i.e.* **TS5**) was found, and this apparently implies involvement of a route similar to **2** → **TS3** → **8** → **5**.

Location of the saddle points allowed an estimate of the activation energies for the addition of formaldoxime to a platinum-bound acetonitrile. Their values relative to the reactants for the mechanism based on the formation of **TS1** and **TS3** are lower than those for routes based on the formation of **TS2** and **TS4** (2.75 vs. 2.93 eV for **TS1** and **TS2**, respectively; 2.63 vs. 2.74 eV for **TS3** and **TS4**). The activation energy is highest for the reaction starting from the platinum(II) complex and lowest for the platinum(IV) neutral species (2.46 eV). Moreover, the reaction energies, estimated as the difference between the total energy of the final complexes **4–6** and the sum of the energies of the starting compounds **1–3** and the oxime in the *A* conformation, are largest in absolute value for the **3** → **6** reaction and smallest for **1** → **4**, *i.e.* –0.69, –0.78 and –0.95 eV for **1**, **2** and **3**. Hence, based on both kinetic (activation energies) and thermodynamic (energetic effects) considerations which are supported by experimental observations, the lowest reactivity towards the addition is expected for the acetonitrile co-ordinated to the platinum(II) centre, while the highest activation by the platinum centre can be predicted for the neutral platinum(IV) species.

The mechanism discussed above is not the only plausible one and others can also be considered, *e.g.* proceeding *via* deprotonation (by a solvent molecule, autoionization or oxime–nitron tautomerization) of the OH group of the oxime and subsequent addition to the metal-bound nitrile followed by protonation of the imino N atom. The deprotonation path can be preferable under base catalysis conditions and is initiated by heterolytic cleavage of the oxime OH bond. Calculations using the 6-31G basis set give for the heterolytic dissociation energy of this bond the value of 16.6 eV which agrees with those (16.0–16.9 eV range) obtained by using more extended basis sets, *i.e.* 6-31G*, DH, TZV, at HF//HF and MP2//MP2 levels. Application of the Kirkwood–Onsager spherical cavity model, to account for the solvent effects, leads to reduction of the dissociation energy which falls in the range from 14.0 (HF/TZV//HF/TZV) to 14.6 eV (HF/6-31G*//HF/6-31G*).

A search for the minima corresponding to the addition products of deprotonated formaldoxime to complexes **1–3**, *i.e.* *trans*-[PtCl₂(MeCN){N=C(Me)ON=CH₂}][–], [PtCl₅{N=C(Me)ON=CH₂}]^{2–} and *trans*-[PtCl₄(MeCN){N=C(Me)ON=CH₂}]^{2–}, was carried out. Two structures which differ in the conformation of the ONCH₂ fragment were located for all platinum(II) and -(IV) species (**10–15**, Fig. 7). In **10**, **11**, **13** and **14** the NC(Me)ONCH₂ fragment is non-planar (the torsion angles NCON and CONC are 69.1 and –20.2° for **13**; –17.2 and 61.0° for **14**), whereas it is planar for **12** and **15**. The search for saddle points was performed from different starting geometries but no TS for the addition of deprotonated formaldoxime to **1–3** was found for all platinum(II) and -(IV) systems and this conceivably implies that this stage of the reaction proceeds without a barrier.

In order to investigate the proton addition in the last step of the reaction, calculations of the electrostatic potential (ESP) distribution for all structures **10–15** were carried out and illustrative examples of the negative ESP maps for **12** and **13** are given in Fig. 8. The most negative ESP is localized near the N(1), N(5), O and Cl atoms providing easiness of N(1) atom protonation. Despite the lone electron pair of N(1) in **12** and **14** being somewhat hindered by the CH₂=NO fragment, protonation might occur due to rotation of the fragment around the C–O and O–N bonds (the rotational barrier is expected to be much lower than the O–H dissociation energy) thus providing an access to the N(1) site.

For the stage of protonation no transition states were found and this fact as well as the ESP distribution pattern suggest that protonation proceeds without overcoming a potential barrier. Thus, in accord with the data presented in

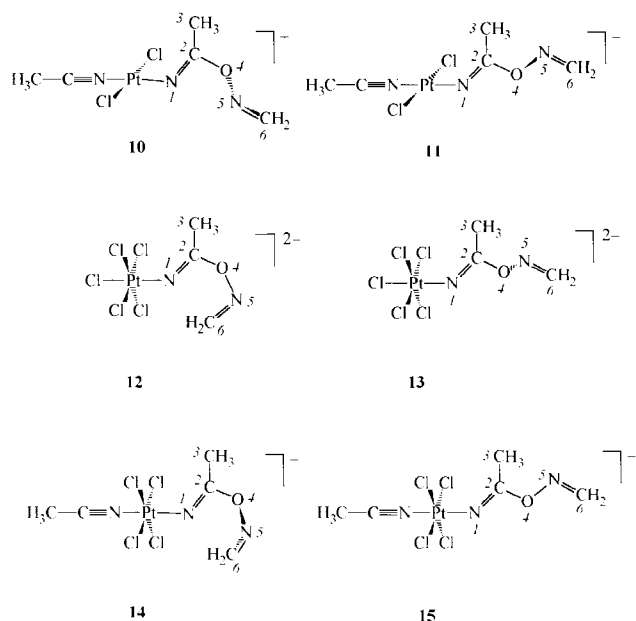


Fig. 7 The structures of the products of addition of deprotonated formaldoxime to complexes 1–3 with numbering of selected atoms.

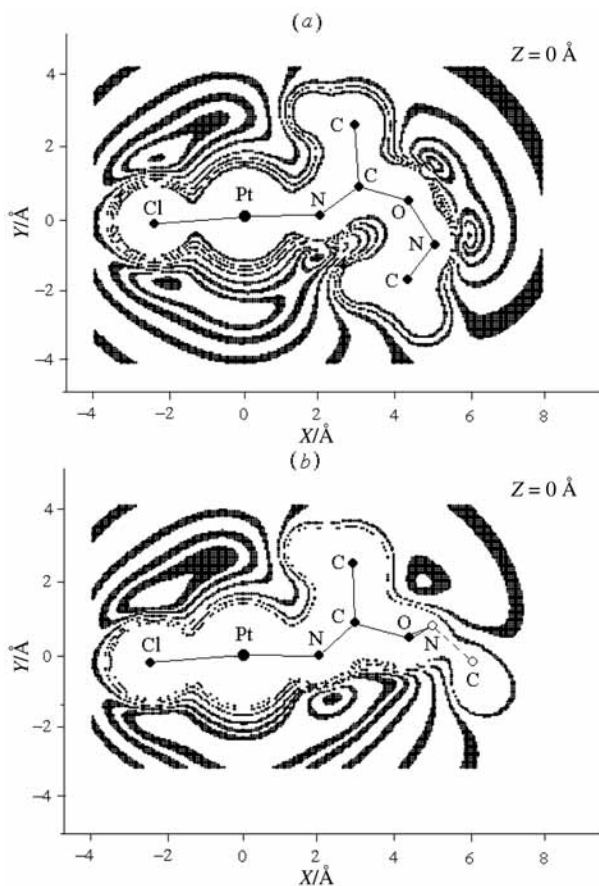


Fig. 8 Distribution of electrostatic potential for structures 12 (a) and 13 (b) in the plane formed by Pt, N(1) and C(2) atoms ($Z = 0 \text{ \AA}$). The four Cl atoms and all H atoms are omitted for clarity.

Fig. 9, the activation barrier for the route discussed, which is determined, in fact, by the dissociation energy of the OH oxime bond, is the same for all complexes 1–3. Under base-catalysed conditions, when deprotonation can be excluded from energy considerations, the energy aspects of the relative reactivity of co-ordinated acetonitrile are determined only by the energies of the starting and final complexes. The negative values of the reaction energy for 1–3 and the absence of

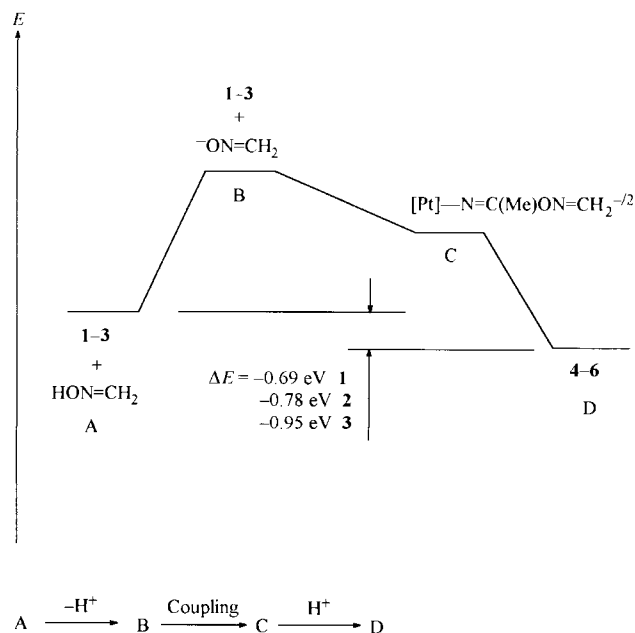


Fig. 9 Energy profile of the reaction of formaldoxime addition to complexes 1–3 (mechanism involving initial deprotonation of the oxime).

potential barriers between levels B and D (Fig. 9) suggest that oxime addition should proceed for both platinum(II) and -(IV) complexes 1–3 and the reactivity should increase from 1 to 3 along with the increase of the absolute value of the reaction energy that is confirmed by the experimental results.

To summarize, our calculations indicate that the reactivity of nitrile towards addition of oxime increases from complex 1 to 3, independently of the mechanism of the reaction, and this conclusion is in full agreement with the experimental data. Moreover, the mechanism based on nucleophilic addition of the undeprotonated oxime is energetically favoured relative to the alternative involving prior deprotonation of oxime (oximate anion then behaving as the nucleophile), unless base-catalysed conditions are effective.

Concluding remarks

The observed relative reactivity of the set of nitrile complexes of this work towards nucleophilic addition of oximes appears to follow the dominant effect of the metal oxidation state which predominates over that of the overall charge of the complexes, since only those of Pt^{IV} undergo such a reaction although, within the reactive ones, that with a negative charge is less reactive than the neutral one. However, the theoretical study indicates that activation of an organonitrile by ligation to a transition metal centre is the result of a delicate balance among a variety of factors that may not be rationalized in terms of simple arguments based on the overall charge of the complex, metal oxidation state, electron donor–acceptor properties of ancillary ligands or even on the LUMO composition or the atomic charges which *e.g.* can show great similarities in complexes with quite different reactivities.

The applied theoretical calculations provided a useful tool for understanding the reaction (which does not appear to be either charge or frontier orbital controlled) in terms of both kinetic (activation energies) and thermodynamic (reaction energies) effects, allowing also the selection of possible pathways. The energetically favoured mechanism involves direct addition, to the activated nitrile ligand, of the protic nucleophile (undeprotonated oxime) in any of its two possible molecular configurations, forming a transition state with a four-membered NCOH ring derived from the interaction of the

oxime OH group with the nitrile N=C moiety. Hydrogen transfer, in this ring, from the former to the latter group followed by further stabilization upon N-H...N hydrogen-bond formation results in the final iminoacylated product presenting the $\text{-N}(\text{H})=\text{C}-\text{O}-\text{N}=\text{C}<$ five-membered ring. Nevertheless, the

least favourable mechanism cannot be ruled out under base-catalysed conditions which would allow prior deprotonation of the oxime (with a much higher energy requirement than that associated with the above "undeprotonation" mechanism) that would be followed by energy favourable oximato-nitrile coupling and protonation steps conceivably proceeding without any potential barrier to overcome.

Water can also behave as a nucleophile leading to the rare conversion, upon hydrolysis in open air under mild conditions, of the activated nitrile into ammonia, at the platinum(IV) anionic species. Hence, the reaction proceeds further than in the case of oximes, resulting in complete cleavage of the N=C bond whereas with the latter nucleophiles the process stops at the intermediate oxime-derived imino (HN=C<) stage which, moreover, is inert towards hydrolysis.

Experimental

Materials and instrumentation

Solvents were obtained from commercial sources and used as received. $[\text{PtCl}_2(\text{EtCN})_2]$ ²⁵ and $[\text{PtCl}_4(\text{NH}_3)(\text{Me}_2\text{SO})]$ ¹⁴ were prepared in accord with published methods. C, H and N elemental analyses were carried out by the Microanalytical Service of the Instituto Superior Técnico. Melting points were determined on a Kofler table. For TLC, Silufol UV 254 SiO₂ plates have been used. Positive-ion FAB mass spectra were obtained on a Trio 2000 instrument by bombarding 3-nitrobenzyl alcohol matrices of the samples with 8 keV (*ca.* 1.28×10^{15} J) Xe atoms. Mass calibration for data system acquisition was achieved using CsI. Infrared spectra (4000–400 cm⁻¹) were recorded on a Bio-Rad FTS 3000MX instrument in KBr pellets, ¹H, ¹³C-¹H, ³¹P-¹H and ¹⁹⁵Pt NMR spectra on a Varian UNITY 300 spectrometer at ambient temperature. ³¹P chemical shifts are quoted relative to H₃PO₄ (δ 0), ¹⁹⁵Pt relative to aqueous K₂[PtCl₄] (δ -1630) and the half height linewidth is given in parentheses. Assignment of the ¹H and ¹³C signals was done by means of COSY and HETCOR experiments.

Synthetic work and characterization

[Ph₃PCH₂Ph][PtCl₃(EtCN)]. A mixture of *cis*- and *trans*- $[\text{PtCl}_2(\text{EtCN})_2]$ (1.00 g, 2.66 mmol) was dissolved on stirring in the minimum amount of chloroform (*ca.* 8 mL) then heated to 50 °C and $[\text{Ph}_3\text{PCH}_2\text{Ph}]\text{Cl}$ (1.05 g, 2.70 mmol) added. The obtained orange-yellow solution was heated to 50 °C for 1 h and then kept at 20–25 °C for 1 d, and large orange crystals were collected on a filter, washed with EtOH (three 3 mL portions) and dried in air at room temperature. Yield of $[\text{Ph}_3\text{PCH}_2\text{Ph}][\text{PtCl}_3(\text{EtCN})]$ 1.03 g, 55%. The filtrate was evaporated to dryness and the residue washed thoroughly with EtOH (three 5 mL portions) to remove the excess of $[\text{Ph}_3\text{PCH}_2\text{Ph}]\text{Cl}$. Yield of additional $[\text{Ph}_3\text{PCH}_2\text{Ph}][\text{PtCl}_3(\text{EtCN})]$ 0.56 g, 30%. The nitrile complex can be recrystallized from an acetone-toluene mixture. Calc. for C₂₈H₂₇Cl₃NPPt: C, 47.37; H, 3.83; Cl, 14.98; N, 1.97. Found: C, 47.21; H, 3.96; Cl, 15.19; N, 2.07%. FAB⁻-MS: *m/z* 356 [M_{anion}], 301 [PtCl₃] and 266 [PtCl₂]. mp = 157 °C. TLC: R_f = 0.43 (eluent acetone-CHCl₃ 1:5). IR spectrum, selected bands (bands in the $\nu(\text{C}\equiv\text{N})$ region are so weak that their attribution is unreliable): 1437s $\nu(\text{C}=\text{C})$, 1111s $\nu(\text{P}-\text{C})$ and 758s cm⁻¹ $\delta(\text{C}-\text{H})$. ¹H NMR in CDCl₃: δ 1.24 (t, *J* 7.2, 3H) and 2.60 (7.5, 2H)(Et), 5.12 (d, ²J_{PH} 14.1 Hz, 2H, CH₂Ph), 7.05 (m, 2H, *ortho*), 7.15 (m, 2H, *meta*) and 7.22 (m, 1H, *para*)(CH₂Ph) and 7.68–7.80 (m, 15H, Ph). ¹³C-¹H

NMR in CDCl₃: δ 9.7 (CH₃) and 12.8 (CH₂)(Et), 30.9 (CH₂, ¹J_{PC} 47.7, CH₂Ph), 117.5 (C_{ipso}, ¹J_{PC} 86.1, Ph), 127.0 (C_{ipso}, ²J_{PC} 9.0, CH₂Ph), 128.4 (CH_p, CH₂Ph), 128.9 (CH_m, CH₂Ph), 130.4 (CH, *J*_{PC} 12.8, Ph), 131.5 (CH_o, *J*_{PC} 5.5, CH₂Ph), 134.3 (CH, *J*_{PC} 9.1 Hz, Ph) and 135.1 (CH_p, Ph); N≡C was not detected. ³¹P-¹H NMR in CDCl₃: δ 23.4. ¹⁹⁵Pt NMR in CDCl₃: δ -2021 (380 Hz).

[Ph₃PCH₂Ph][PtCl₅(EtCN)]. The complex was obtained by oxidation of $[\text{Ph}_3\text{PCH}_2\text{Ph}][\text{PtCl}_3(\text{EtCN})]$ with Cl₂ in chloroform by use of a standard procedure.⁴ Calc. for C₂₈H₂₇Cl₅NPPt: C, 43.07; H, 3.49; Cl, 22.70; N, 1.79. Found: C, 43.05; H, 3.52; Cl, 22.13; N, 1.77%. FAB⁻-MS: *m/z* 428 [M_{anion}], 373 [PtCl₅], 336 [PtCl₄], 301 [PtCl₃] and 266 [PtCl₂]. mp = 155 °C. TLC: R_f = 0.40 (eluent acetone-CHCl₃ 1:3). IR spectrum in KBr, selected bands: 2327m $\nu(\text{C}\equiv\text{N})$, 1438s (C=C), 1111s (P-C) and 755s cm⁻¹ $\delta(\text{C}-\text{H})$. ¹H NMR in CDCl₃: δ 1.31 (t, 7.5 Hz, 3H) and 2.85 (q, *J* 7.5, 2H)(Et), 4.88 (d, ²J_{PH} 13.8 Hz, 2H, CH₂Ph), 7.03 (m, 2H, *ortho*), 7.13 (m, 2H, *meta*) and 7.24 (m, 1H, *para*)(CH₂Ph), 7.53–7.69 (m, 12H, *ortho* + *meta*) and 7.77 (m, 3H, *para*)(Ph). ¹³C-¹H NMR in CDCl₃: δ 9.5 (CH₃) and 12.9 (CH₂)(Et), 31.3 (CH₂, ¹J_{PC} 48.6, CH₂Ph), 117.2 (C_{ipso}, ¹J_{PC} 86.0, Ph), 126.9 (C_{ipso}, ²J_{PC} 8.8, CH₂Ph), 128.6 (CH_p, CH₂Ph), 128.9 (CH_m, CH₂Ph), 130.4 (CH, *J*_{PC} 12.8, Ph), 131.6 (CH_o, *J*_{PC} 5.3, CH₂Ph), 134.3 (CH, *J*_{PC} 10.1 Hz, Ph) and 135.2 (CH_p, Ph); N≡C was not detected. ³¹P-¹H NMR in CDCl₃: δ 23.3. ¹⁹⁵Pt NMR in CDCl₃: δ -184 (170 Hz).

Independent synthesis of [Ph₃PCH₂Ph][PtCl₅(NH₃)]. $[\text{Ph}_3\text{PCH}_2\text{Ph}]\text{Cl}$ (0.18 g, 0.46 mmol) was added to a suspension of $[\text{PtCl}_4(\text{NH}_3)(\text{Me}_2\text{SO})]$ in chloroform (8 mL) then heated at 50–60 °C for 30 min. During that time the reaction mixture was homogenized in a few minutes and a yellow precipitate formed. The new suspension was cooled to room temperature and the precipitate filtered off, washed with two 3 mL portions of chloroform and dried in air at room temperature. Yield of $[\text{Ph}_3\text{PCH}_2\text{Ph}][\text{PtCl}_5(\text{NH}_3)]$ 0.29 g, 85%. Calc. for C₂₅H₂₅Cl₅NPPt: C, 40.42; H, 3.39; Cl, 23.86; N, 1.89. Found: C, 39.60; H, 3.38; Cl, 23.80; N, 1.90%. FAB⁻-MS: *m/z* 390 [M_{anion}], 373 [PtCl₅], 336 [PtCl₄], 301 [PtCl₃] and 266 [PtCl₂]. mp = 218 °C (decomp.). TLC: R_f = 0.32 (eluent acetone-CHCl₃ 1:3). IR spectrum in KBr, selected bands: 3290m and 3188m-w $\nu(\text{N}-\text{H})$, 1437s $\nu(\text{C}=\text{C})$, 1111s $\nu(\text{P}-\text{C})$ and 746s cm⁻¹ $\delta(\text{C}-\text{H})$. ¹H NMR in DMSO-*d*₆: δ 5.14 (d, ²J_{PH} 15.6, 2H, CH₂Ph), 5.55 (triplet each line having platinum satellites, *J*_{H¹⁹⁵N} 53, *J*_{PH} 52, 3H, NH₃), 6.97 (d, 7.2 Hz, 2H, *ortho*), 7.22 (t, *J* 7.5, 2H, *meta*) and 7.27 (m, 1H, *para*)(CH₂Ph), 7.75 (m, 12H, *ortho* + *meta*) and 7.90 (t, *J* 7.8 Hz, 3H, *para*)(Ph). ¹³C-¹H NMR in DMSO-*d*₆: δ 28.1 (CH₂, ¹J_{PC} 48), 117.8 (C_{ipso}, ¹J_{PC} 86, Ph), 127.9 (C_{ipso}, ²J_{PC} 8.2, CH₂Ph), 128.6 (CH_m, CH₂Ph), 128.9 (CH_p, CH₂Ph), 130.1 (CH, *J*_{PC} 12.8, Ph), 131.0 (CH_o, *J* 4.0, CH₂Ph), 134.0 (CH, *J*_{PC} 9.1 Hz, Ph) and 135.1 (CH_p, Ph). ³¹P-¹H NMR in DMSO-*d*₆: δ 28.3. ¹⁹⁵Pt-¹H NMR in DMSO-*d*₆: δ 91 (t, *J*_{H¹⁹⁵N} 169 Hz). ¹⁹⁵Pt NMR in DMSO-*d*₆: δ 91 (tq, *J*_{H¹⁹⁵N} 169, *J*_{PH} 52 Hz).

Reaction of [Ph₃PCH₂Ph][PtCl₅(EtCN)] with ketoximes and amidoxime (Me₂C=NOH, (C₆H₁₀)C=NOH, (C₉H₁₈)C=NOH, (C₄H₈)C=NOH, (C₅H₁₀)C=NOH or PhC(NH₂)=NOH). In a typical experiment, $[\text{Ph}_3\text{PCH}_2\text{Ph}][\text{PtCl}_5(\text{EtCN})]$ (0.05 g, 0.09 mmol) was suspended in chloroform (6 mL), the oxime (0.10 mmol) added and the reaction mixture left to stand with stirring at room temperature for 2–3 d. The completeness of the reaction was confirmed by TLC whereafter the yellow solution formed was evaporated to dryness and washed with five 3 mL portions of diethyl ether to remove the excess of oxime. Yields 80–90%.

[Ph₃PCH₂Ph][PtCl₅{NH=C(Et)ON=CMe₂}]. Calc. for C₃₁H₃₄Cl₅N₂OPPt: C, 43.60; H, 4.01; Cl, 20.76; N, 3.28. Found: C, 42.85; H, 4.11; Cl, 20.42; N, 3.19%. FAB⁻-MS: *m/z* 498 [M_{anion}].

373 [PtCl₅], 336 [PtCl₄], 301 [PtCl₃] and 266 [PtCl₂]. mp = 144 °C. TLC: *R_f* = 0.65 (eluent acetone–CHCl₃ 1:3). IR spectrum in KBr, selected bands: 3299m ν(N–H), 1656 and 1630s ν(C=N), 1439s ν(C=C), 1111s ν(P–C) and 747s cm⁻¹ δ(C–H). ¹H NMR in CDCl₃: δ 1.20 (t, *J* 7.4, 3H) and 3.23 (q, *J* 7.8 Hz, 2H)(Et), 2.00 (s, 3H) and 2.02 (s, 3H)(oxime), 4.92 (s, broad, 2H, CH₂Ph), 7.05 (m, 2H, *ortho*), 7.13 (m, 2H, *meta*) and 7.24 (m, 1H, *para*)(CH₂Ph), 7.65 (m, 12H, *ortho* + *meta*) and 7.76 (m, 3H, *para*)(Ph) and 8.60 (s, broad, 1H, NH). ¹³C-¹H} NMR in CDCl₃: δ 10.6 (CH₃) and 25.0 (CH₂)(Et), 17.3 (CH₃) and 21.9 (CH₃)(oxime), 32.4 (CH₂, ¹*J*_{PC} 49.6, CH₂Ph), 117.4 (*C*_{ipso}, ¹*J*_{PC} 86.0, Ph), 126.8 (*C*_{ipso}, ²*J*_{PC} 8.4, CH₂Ph), 128.6 (CH_p, CH₂Ph), 128.9 (CH_m, CH₂Ph), 130.5 (CH, *J*_{PC} 11.9, Ph), 131.8 (CH_o, *J*_{PC} 4.8, CH₂Ph), 134.6 (CH, *J*_{PC} 8.9 Hz, Ph), 135.2 (CH_p, Ph), 165.0 (N=C) and 175.8 (HN=C). ³¹P-¹H} NMR in CDCl₃: δ 23.6. ¹⁹⁵Pt NMR in CDCl₃: δ +1.5 (440 Hz).

[Ph₃PCH₂Ph][PtCl₅{NH=C(Et)ON=C(C₄H₈)}]. Calc. for C₃₃H₃₆Cl₅N₂OPPt: C, 45.04; H, 4.12; Cl, 20.14; N, 3.18. Found: C, 44.87; H, 4.04; Cl, 20.31; N, 3.25%. FAB⁻-MS: *m/z* 524 [M_{anion}], 373 [PtCl₅], 336 [PtCl₄], 301 [PtCl₃] and 266 [PtCl₂]. mp = 153 °C. TLC: *R_f* = 0.65 (eluent acetone–CHCl₃ 1:3). IR spectrum in KBr, selected bands: 3294m-w ν(N–H), 1640s ν(C=N), 1438s ν(C=C), 1111s ν(P–C) and 748s cm⁻¹ δ(C–H). ¹H NMR in CDCl₃: δ 1.20 (t, *J* 7.5, 3H) and 3.23 (q, *J* 7.5, 2H)(Et), 1.83 (m, 4H), 2.50 (t, *J* 6.9, 2H) and 2.57 (t, *J* 7.0, 2H)(oxime), 4.95 (d, ²*J*_{PH} 12.9 Hz, 2H, CH₂Ph), 7.05 (m, 2H, *ortho*), 7.14 (m, 2H, *meta*) and 7.24 (m, 1H, *para*)(CH₂Ph), 7.64 (m, 6H, *ortho* or *meta*), 7.67 (m, 6H, *ortho* or *meta*) and 7.78 (m, 3H, *para*)(Ph) and 8.59 (s, broad, 1H, NH). ¹³C-¹H} NMR in CDCl₃: δ 10.6 (CH₃) and 25.0 (CH₂)(Et), 24.4 (CH₂), 25.1 (CH₂), 29.6 (CH₂) and 31.5 (CH₂)(oxime), 31.5 (CH₂, ¹*J*_{PC} 47.7, CH₂Ph), 117.4 (*C*_{ipso}, ¹*J*_{PC} 86.1, Ph), 126.9 (*C*_{ipso}, ²*J*_{PC} 10.1, CH₂Ph), 128.5 (CH_p, CH₂Ph), 128.9 (CH_m, CH₂Ph), 130.3 (CH, *J*_{PC} 12.8, Ph), 131.6 (CH_o, *J*_{PC} 5.5, CH₂Ph), 134.4 (CH, *J*_{PC} 9.2 Hz, Ph), 135.1 (CH_p, Ph), 176.0 (HN=C) and 176.5 (N=C, oxime). ³¹P-¹H} NMR in CDCl₃: δ 23.4. ¹⁹⁵Pt NMR in CDCl₃: δ +0.8 (280 Hz).

[Ph₃PCH₂Ph][PtCl₅{NH=C(Et)ON=C(C₅H₁₀)}]. Calc. for C₃₄H₃₈Cl₅N₂OPPt: C, 45.68; H, 4.28; Cl, 19.83; N, 3.13. Found: C, 45.22; H, 4.28; Cl, 20.18; N, 3.18%. FAB⁻-MS: *m/z* 540 [M_{anion} – H]⁺, 373 [PtCl₅], 336 [PtCl₄], 301 [PtCl₃] and 266 [PtCl₂]. mp = 145 °C. TLC: *R_f* = 0.67 (eluent acetone–CHCl₃ = 1:3). IR spectrum in KBr, selected bands: 3285m-w ν(N–H), 1638s ν(C=N), 1438s ν(C=C), 1112s ν(P–C) and 749s cm⁻¹ δ(C–H). ¹H NMR in CDCl₃: δ 1.21 (t, *J* 7.5, 3H) and 3.24 (q, *J* 7.2, 2H)(Et), 1.71 (m, 6H), 2.32 (m, 2H) and 2.55 (m, 2H)(oxime), 4.92 (d, ²*J*_{PH} 11.4 Hz, 2H, CH₂Ph), 7.04 (m, 2H, *ortho*), 7.14 (m, 2H, *meta*) and 7.24 (m, 1H, *para*)(CH₂Ph), 7.67 (m, 12H, *ortho* + *meta*) and 7.78 (m, 3H, *para*)(Ph) and 8.66 (s, broad, 1H, NH). ¹³C-¹H} NMR in CDCl₃: δ 10.6 (CH₃) and 25.1 (CH₂)(Et), 25.2 (CH₂), 25.8 (CH₂), 26.7 (CH₂), 27.1 (CH₂) and 31.9 (CH₂)(oxime), 32.4 (CH₂, ¹*J*_{PC} 45.0, CH₂Ph), 117.4 (*C*_{ipso}, ¹*J*_{PC} 85.2, Ph), 126.8 (*C*_{ipso}, ²*J*_{PC} 8.0, CH₂Ph), 128.5 (CH_p, CH₂Ph), 128.9 (CH_m, *J*_{PC} 2.0, CH₂Ph), 130.4 (CH, *J*_{PC} 12.8, Ph), 131.7 (CH_o, *J*_{PC} 5.3, CH₂Ph), 134.4 (CH, *J*_{PC} 10.1 Hz, Ph), 135.1 (CH_p, Ph), 176.0 (HN=C) and 169.7 (N=C, oxime). ³¹P-¹H} NMR in CDCl₃: δ 23.4. ¹⁹⁵Pt NMR in CDCl₃: δ +2.6 (360 Hz).

[Ph₃PCH₂Ph][PtCl₅{NH=C(Et)ON=C(C₉H₁₆)}]. Calc. for C₃₈H₄₄Cl₅N₂OPPt: C, 48.14; H, 4.68; Cl, 18.69; N, 2.96. Found: C, 47.77; H, 4.51; Cl, 18.45; N, 3.03%. FAB⁻-MS: *m/z* 595 [M_{anion}], 373 [PtCl₅], 336 [PtCl₄], 301 [PtCl₃] and 266 [PtCl₂]. mp = 155 °C. TLC: *R_f* = 0.67 (eluent acetone–CHCl₃ = 1:3). IR spectrum in KBr, selected bands: 3277m-w ν(N–H), 1646s ν(C=N), 1438s ν(C=C), 1112s ν(P–C) and 751s cm⁻¹ δ(C–H). ¹H NMR in CDCl₃: δ 1.20 (t, *J* 7.5, 3H) and 3.25 (m, 2H)(Et), 0.80 (s, 3H) and 0.94 (s, 3H)(H-9, H-10), 1.04 (s, 3H, 8-H), 1.25 (m, 1H), 1.46 (m, 1H), 1.77 (m, 1H) and 1.84 (m, 1H)(H-5, H-6), 1.98 (m, H-4), 2.13 (d, *J* 12.0, 1H, H-3 *endo*), 2.64 (dm, *J* 12.0, 1H, H-3 *exo*)(oxime), 4.91 (d, ²*J*_{PH} 8.8 Hz, 2H, CH₂Ph), 7.04 (m, 2H, *ortho*), 7.14 (m, 2H, *meta*) and 7.24 (m, 1H,

para)(CH₂Ph), 7.59 (m, 6H, *ortho* or *meta*), 7.67 (m, 6H, *ortho* or *meta*) and 7.76 (m, 3H, *para*)(Ph) and 8.60 (s, broad, 1H, NH). ¹³C-¹H} NMR in CDCl₃: δ 10.6 (CH₃) and 25.1 (CH₂, ³*J*_{PC} 9.5)(Et), 10.8 (CH₃, C-8), 18.4 (CH₃) and 19.5 (CH₃)(C-9, C-10), 26.9 (CH₂) and 32.3 (CH₂)(C-5, C-6), 34.9 (CH₂, C-3), 43.4 (CH, C-4), 48.9 (C, C-7) and 53.7 (C, C-1)(oxime), 31.5 (CH₂, ¹*J*_{PC} 47.6, CH₂Ph), 117.4 (*C*_{ipso}, ¹*J*_{PC} 86.0, Ph), 126.9 (*C*_{ipso}, ²*J*_{PC} 8.1, CH₂Ph), 128.5 (CH_p, CH₂Ph), 128.9 (CH_m, *J*_{PC} 2.3, CH₂Ph), 130.4 (CH, *J*_{PC} 12.0, Ph), 131.6 (CH_o, *J*_{PC} 5.5, CH₂Ph), 134.5 (CH, *J*_{PC} 10.1 Hz, Ph), 135.1 (CH_p, Ph), 176.1 (HN=C) and 178.6 (N=C, oxime). ³¹P-¹H} NMR in CDCl₃: δ 23.4. ¹⁹⁵Pt NMR in CDCl₃: δ -0.1 (320 Hz).

[Ph₃PCH₂Ph][PtCl₅{NH=C(Et)ON=C(C₉H₁₈)}]. Calc. for C₃₈H₄₆Cl₅N₂OPPt: C, 48.04; H, 4.88; Cl, 18.66; N, 2.95. Found: C, 48.02; H, 4.76; Cl, 18.50; N, 2.89%. FAB⁻-MS: *m/z* 597 [M_{anion}], 373 [PtCl₅], 336 [PtCl₄], 301 [PtCl₃] and 266 [PtCl₂]. mp = 83 °C. TLC: *R_f* = 0.67 (eluent acetone–CHCl₃ = 1:3). IR spectrum in KBr, selected bands: 3279m-w ν(N–H), 1630s ν(C=N), 1438s ν(C=C), 1111s ν(P–C) and 750s cm⁻¹ δ(C–H). ¹H NMR in CDCl₃: δ 1.22 (t, *J* 7.2, 3H), 3.18 (dq, *J* 6.2, 7.5, 1H) and 3.31 (dq, *J* 16.5, 7.5, 1H)(Et), 0.91 (d, *J* 6.6, 3H) and 0.94 (d, *J* 6.3, 3H)(H-8, H-9), 0.99 (d, 5.7 Hz, 3H, H-10), 1.22 (m, 1H, H-4 ax.), 1.48 (q m, *J* 10.2, 1H, H-3 ax.), 1.86 (m, 1H, 5-H), 1.88 (m, 1H, H-4 eq.), 1.92 (m, 1H, H-6 ax.), 1.96 (m, 1H, H-3 eq.), 2.06 (m, 1H, H-2), 2.15 (sept, *J* 6.6, 1H, H-7), 2.87 (dm, *J* 10.5, 1H, H-6 eq.)(oxime), 4.91 (d, ²*J*_{PH} 12.6 Hz, 2H, CH₂Ph), 7.04 (m, 2H, *ortho*), 7.14 (m, 2H, *meta*) and 7.24 (m, 1H, *para*)(CH₂Ph), 7.66 (m, 12H, *ortho* + *meta*) and 7.77 (m, 3H, *para*)(Ph) and 8.72 (s, broad, 1H, NH). ¹³C-¹H} NMR in CDCl₃: δ 10.5 (CH₃) and 24.9 (CH₂, ³*J*_{PC} 5.5)(Et), 19.3 (CH₃, C-8 or C-9), 21.1 (CH₃, C-10), 21.5 (CH₃, C-8 or C-9), 26.5 (CH, C-7), 26.9 (CH₂, C-3), 31.7 (CH₂, C-4), 32.9 (CH, C-5), 34.1 (CH₂, C-6) and 49.3 (CH, C-2)(oxime), 31.7 (CH₂, ¹*J*_{PC} 47.0, CH₂Ph), 117.4 (*C*_{ipso}, ¹*J*_{PC} 85.2, Ph), 126.9 (*C*_{ipso}, ²*J*_{PC} 8.7, CH₂Ph), 128.5 (CH_p, CH₂Ph), 128.9 (CH_m, CH₂Ph), 130.4 (CH, *J*_{PC} 12.8, Ph), 131.7 (CH_o, *J*_{PC} 4.7, CH₂Ph), 134.5 (CH, *J*_{PC} 10.0 Hz, Ph), 135.1 (CH_p, Ph), 170.7 (N=C, oxime) and 176.0 (HN=C). ³¹P-¹H} NMR in CDCl₃: δ 23.4. ¹⁹⁵Pt NMR in CDCl₃: δ -2.0 (320 Hz).

[Ph₃PCH₂Ph][PtCl₅{NH=C(Et)ON=C(NH₂)Ph}]. Calc. for C₃₅H₃₅Cl₅N₃OPPt: C, 45.84; H, 3.85; Cl, 19.39; N, 4.58. Found: C, 46.33; H, 3.70; Cl, 19.01; N, 4.82%. FAB⁻-MS: *m/z* 563 [M_{anion}], 372 [PtCl₅], 336 [PtCl₄], 301 [PtCl₃] and 266 [PtCl₂]. mp = 117–120 °C. TLC: *R_f* = 0.43 (eluent acetone–CHCl₃ = 1:3). IR spectrum in KBr, selected bands: 3430m-w ν(NH₂), 3349m-w ν(NH₂), 3265m-w ν(N–H), 1623s ν(C=N), 1437s ν(C=C), 1111s ν(P–C) and 750s cm⁻¹ δ(C–H). ¹H NMR in CDCl₃: δ 1.11 (t, *J* 7.2, 3H) and 3.10 (q, *J* 7.5, 1H)(Et), 4.72 (d, ²*J*_{PH} 14.4 Hz, 2H, CH₂Ph), 5.87 (s, broad, 2H, NH₂), 6.81 (m, 2H, *ortho*), 6.91 (m, 2H, *meta*) and 7.01 (m, 1H, *para*)(CH₂Ph), 7.17 (m, 3H, Ph amidoxime), 7.44 (m, 12H, *ortho* + *meta*) and 7.58 (m, 3H, *para*)(Ph), 7.67 (m, 2H, Ph amidoxime) and 8.64 (s, broad, 1H, NH). ¹³C-¹H} NMR in CDCl₃: δ 10.8 (CH₃) and 24.6 (CH₂, ³*J*_{PC} 4.8)(Et), 30.6 (CH₂, ¹*J*_{PC} 48.0, CH₂Ph), 117.2 (*C*_{ipso}, ¹*J*_{PC} 86.0, Ph), 126.8 (*C*_{ipso}, ²*J*_{PC} 8.5, CH₂Ph), 127.3 (Ph amidoxime), 128.1 (Ph amidoxime), 128.4 (CH_p, CH₂Ph), 128.7 (CH_m, CH₂Ph), 129.0 (Ph amidoxime), 130.0 (CH, *J*_{PC} 12.8, Ph), 131.0 (Ph amidoxime), 131.2 (CH_p, *J*_{PC} 5.5, CH₂Ph), 134.1 (CH, *J*_{PC} 10.0 Hz, Ph), 134.9 (CH_p, Ph), 156.9 (N=C, amidoxime) and 175.5 (HN=C). ³¹P-¹H} NMR in CDCl₃: δ 23.2. ¹⁹⁵Pt NMR in CDCl₃: δ +19.9 (400 Hz).

Structure determination of [Ph₃PCH₂Ph][PtCl₅{NH=C(Et)ON=C(C₉H₁₆)}].

Yellow prisms of the complex were obtained directly from the reaction mixture. Diffraction data were collected on an Enraf-Nonius CAD 4 diffractometer. Data processing was performed using the program PROFIT.²⁶ The structure was solved using the SHELXTL package²⁷ by means of Fourier synthesis based

Table 3 Crystal data and structure refinement for [Ph₃PCH₂Ph]₂[PtCl₅(NH=C(Et)ON=C(C₉H₁₆))]

Empirical formula	C ₃₈ H ₄₄ Cl ₅ N ₂ OPt
Formula weight	948.12
<i>T</i> /K	293(2)
Crystal system, space group	Monoclinic, <i>P</i> ₂ ₁ (no. 4)
<i>a</i> /Å	15.379(3)
<i>b</i> /Å	11.402(2)
<i>c</i> /Å	23.776(5)
β /°	100.94(3)
<i>V</i> /Å ³	4093.4(14)
<i>Z</i>	4
μ /mm ⁻¹	3.8
Reflections collected/unique	3820/3676 [<i>R</i> _{int} = 0.053]
Final <i>R</i> ₁ , <i>wR</i> ₂ [<i>I</i> > 2 σ (<i>I</i>)]	0.0436, 0.1185
(all data)	0.0436, 0.1185

on the coordinates of the Pt atom obtained from Patterson synthesis. All reflections with $I \leq 2\sigma(I)$ were then excluded from calculations. Refinement was done by full-matrix least squares based on F^2 using the SHELXL 97 package.²⁸ All non-H atoms were treated anisotropically. An extinction correction has been applied. Lorentz, polarization, and absorption correction were made.²⁹ Scattering factors from ref. 30. Crystal data are given in Table 3.

CCDC reference number 186/2227.

See <http://www.rsc.org/suppdata/dt/b0/b006168i/> for crystallographic files in .cif format.

Computational details

The full geometry optimization of all structures and transition states has been carried out in Cartesian coordinates using the quasi-Newton–Raphson gradient method and the restricted Hartree–Fock approximation by use of the GAMESS program package.³¹ Symmetry operations were not applied. As the quantum-chemical calculations of compounds with heavy 5d and 6d elements should use a relativistic quantum mechanic approach, the Stuttgart quasi-relativistic pseudopotential for 60 core electrons and the appropriate contracted basis set for the platinum atom³² have been used. The standard basis set of Gauss functions 6-31G^{33,34} was selected for all other atoms and d-type polarization functions with exponent 0.75^{34,35} were added for the Cl atoms. Such a basis set is denoted as I. The geometry optimization of formaldoxime and starting complexes has been performed also applying other basis sets for non-Pt atoms (3-21G,³⁶ 6-31G*,^{34,35} DH,³⁷ TZV³⁸). Full geometry optimization was carried out for one of the starting complexes and for formaldoxime taking into account electron correlation effects at the second-order Møller–Plesset perturbation (MP2) level of theory.³⁹ The Hessian matrix was calculated numerically for all structures in order to confirm the location of correct minima or saddle points. All structures calculated at HF level are either minima (there are no imaginary frequencies) or transition states (there is only one negative eigenvalue) on the potential surface.

The intrinsic reaction path was also calculated for one of the reactions by the Gonzalez–Schlegel method.⁴⁰ The calculations were started from the found saddle points to the direction in which the largest magnitude component of the imaginary normal mode is positive and to the opposite direction. Solvent effects were taken into account for formaldoxime using the Kirkwood–Onsager spherical cavity model⁴¹ with CH₂Cl₂ as solvent, the dielectric constant (relative permittivity) was taken as 9.08 and the cavity radius was calculated from the density (1.325 g cm⁻³).

The electrostatic potential distribution for the products of addition of deprotonated formaldoxime to the starting platinum complexes was calculated for the grid of points in the plane formed by Pt, N and C nitrile atoms (nitrile ligand

participated in the reaction) and in the parallel planes (at distances of 1, 2 and 3 Å from the former plane) with step points of 0.05 Å.

Acknowledgements

M. L. K. and G. W. are grateful to the PRAXIS XXI program for fellowships (BPD16369/98 and BPD11779/97). V. Yu. K. is very much obliged to INTAS (grant 97-0166) and the PRAXIS XXI program (grant BCC16428/98) for financial support of this study. V. Yu. K. and T. P. thank the Nordic Council of Ministers for the grant. A. J. L. P. thanks the FCT (Foundation for Science and Technology) and the PRAXIS XXI program (Portugal) for financial support. The authors are indebted to Professor V. K. Belsky (L. Ya. Karpov Physicochemical Institute, Moscow) for the crystal structure determination.

References

- 1 E. C. Constable, *Metals and Ligand Reactivity. An Introduction to the Organic Chemistry of Metal Complexes*, VCH, Weinheim, 1995, p. 65; J. A. Davies, C. M. Hockensmith, V. Yu. Kukushkin and Yu. N. Kukushkin, *Synthetic Coordination Chemistry: Theory and Practice*, World Scientific, Singapore, 1996, 452 pp.
- 2 For reviews see: V. Yu. Kukushkin and A. J. L. Pombeiro, *Coord. Chem. Rev.*, 1999, **181**, 147; V. Yu. Kukushkin, D. Tudela and A. J. L. Pombeiro, *Coord. Chem. Rev.*, 1996, **156**, 333.
- 3 V. Yu. Kukushkin, T. Nishioka, D. Tudela, K. Isobe and I. Kinoshita, *Inorg. Chem.*, 1997, **36**, 6157; V. Yu. Kukushkin, V. K. Belsky and D. Tudela, *Inorg. Chem.*, 1996, **35**, 510; V. Yu. Kukushkin, D. Tudela, Y. A. Izotova, V. K. Belsky and A. I. Stash, *Inorg. Chem.*, 1996, **35**, 4926; V. Yu. Kukushkin, V. K. Belsky, E. A. Aleksandrova, V. E. Konovalov and G. A. Kirakosyan, *Inorg. Chem.*, 1992, **31**, 3836; C. M. P. Ferreira, M. F. C. Guedes da Silva, V. Yu. Kukushkin, J. J. R. Fraústo da Silva and A. J. L. Pombeiro, *J. Chem. Soc., Dalton Trans.*, 1998, 325.
- 4 V. Yu. Kukushkin, T. B. Pakhomova, Yu. N. Kukushkin, R. Herrmann, G. Wagner and A. J. L. Pombeiro, *Inorg. Chem.*, 1998, **37**, 6511; V. Yu. Kukushkin, T. B. Pakhomova, N. A. Bokach, G. Wagner, M. L. Kuznetsov, M. Galanski and A. J. L. Pombeiro, *Inorg. Chem.*, 2000, **39**, 216.
- 5 V. Yu. Kukushkin, T. Nishioka, S. Nakamura, I. Kinoshita and K. Isobe, *Chem. Lett.*, 1997, 189; Yu. N. Kukushkin, N. P. Kiseleva, E. Zangrando and V. Yu. Kukushkin, *Inorg. Chim. Acta*, 1999, **285**, 203; M. F. C. Guedes da Silva, C. M. P. Ferreira, E. M. P. R. P. Branco, J. J. R. Fraústo da Silva, A. J. L. Pombeiro, R. A. Michelin, U. Belluco, R. Bertani, M. Mozzon, G. Bombieri, F. Benetollo and V. Yu. Kukushkin, *Inorg. Chim. Acta*, 1997, **265**, 267; A. J. L. Pombeiro, D. L. Hughes and R. L. Richards, *J. Chem. Soc., Chem. Commun.*, 1988, 1052; A. J. L. Pombeiro, *New J. Chem.*, 1994, **18**, 163; M. F. C. Guedes da Silva, J. J. R. Fraústo da Silva and A. J. L. Pombeiro, *J. Chem. Soc., Dalton Trans.*, 1994, 3299; M. F. C. Guedes da Silva, J. J. R. Fraústo da Silva, A. J. L. Pombeiro, C. Amatore and J.-N. Verpeaux, *Organometallics*, 1994, **13**, 3943; M. F. C. Guedes da Silva, J. J. R. Fraústo da Silva, A. J. L. Pombeiro, C. Amatore and J.-N. Verpeaux, *Inorg. Chem.*, 1998, **37**, 2344; L. M. D. R. S. Martins, M. T. Duarte, A. M. Galvão, C. Resende, A. J. L. Pombeiro, R. A. Henderson and D. J. Evans, *J. Chem. Soc., Dalton Trans.*, 1998, 3311; V. Yu. Kukushkin, I. V. Ilichev, G. Wagner, M. D. Revenco, V. H. Kravtsov and K. Suwinska, *Eur. J. Inorg. Chem.*, 2000, 1315.
- 6 G. Wagner, A. J. L. Pombeiro and V. Yu. Kukushkin, *J. Am. Chem. Soc.*, 2000, **122**, 3106.
- 7 R. A. Michelin, M. Mozzon and R. Bertani, *Coord. Chem. Rev.*, 1996, **147**, 299.
- 8 R. Ros, J. Renaud and R. Roulet, *J. Organomet. Chem.*, 1976, **104**, 271; Yu. N. Kukushkin and Yu. E. Larionova, *Zh. Obshch. Khim.*, 1994, **64**, 1409.
- 9 H.-G. Ang, C.-H. Koh, L.-L. Koh, W.-L. Kwik, W.-K. Leong and W.-Y. Leong, *J. Chem. Soc., Dalton Trans.*, 1993, 847; F. A. Cotton, L. M. Daniels, C. A. Murillo and X. Wang, *Polyhedron*, 1998, **17**, 2781; F. A. Cotton and F. E. Kühn, *J. Am. Chem. Soc.*, 1996, **118**, 5826.
- 10 G. Wagner, A. J. L. Pombeiro, N. A. Bokach and V. Yu. Kukushkin, *J. Chem. Soc., Dalton Trans.*, 1999, 4083.
- 11 V. Yu. Kukushkin, I. V. Ilichev, G. Wagner, J. J. R. Fraústo da Silva and A. J. L. Pombeiro, *J. Chem. Soc., Dalton Trans.*, 1999, 3047;

- V. Yu. Kukushkin, I. V. Ilchev, M. A. Zhdanova, G. Wagner and A. J. L. Pombeiro, *J. Chem. Soc., Dalton Trans.*, 2000, 1567.
- 12 C. M. P. Ferreira, M. F. C. Guedes da Silva, J. J. R. Fraústo da Silva, A. J. L. Pombeiro, V. Yu. Kukushkin and R. A. Michelin, *Inorg. Chem.*, in press.
- 13 V. Yu. Kukushkin, I. A. Krol, Z. A. Starikova and V. M. Tkachuk, *Koord. Khim.*, 1990, **16**, 1406; V. Yu. Kukushkin, I. A. Krol, Z. A. Starikova and V. M. Tkachuk, *Sov. Coord. Chem. (Engl. Transl.)*, 1990, **16**, 746.
- 14 V. Yu. Kukushkin, A. I. Moiseev and E. O. Sidorov, *Zh. Obshch. Khim.*, 1989, **59**, 1958; V. Yu. Kukushkin, V. K. Belsky, E. A. Aleksandrova, E. Yu. Pankova, V. E. Konovalov, V. N. Yakovlev and A. I. Moiseev, *Zh. Obshch. Khim.*, 1991, **61**, 318; V. Yu. Kukushkin, V. K. Belsky, E. A. Aleksandrova, E. Yu. Pankova, V. E. Konovalov, V. N. Yakovlev and A. I. Moiseev, *J. Gen. Chem. (Engl. Transl.)*, 1991, **61**, 284; V. K. Belsky, V. Yu. Kukushkin, V. E. Konovalov, A. I. Moiseev and V. N. Yakovlev, *Zh. Obshch. Khim.*, 1990, **60**, 2180; V. K. Belsky, V. Yu. Kukushkin, V. E. Konovalov, A. I. Moiseev and V. N. Yakovlev, *J. Gen. Chem. (Engl. Transl.)*, 1990, **60**, 1947.
- 15 R. C. Larock, *Comprehensive Organic Transformations. A Guide to Functional Group Preparations*, VCH, Weinheim, 1989, p. 993.
- 16 V. Yu. Kukushkin, I. G. Zenkevich, V. K. Belsky, V. E. Konovalov, A. I. Moiseev and E. O. Sidorov, *Inorg. Chim. Acta*, 1989, **166**, 79.
- 17 G. R. Lee and J. A. Crayston, *Polyhedron*, 1996, **15**, 1817.
- 18 R. Cini, F. P. Intini, L. Maresca, C. Pacifico and G. Natile, *Eur. J. Inorg. Chem.*, 1998, 1305 and references therein.
- 19 S. J. Anderson, P. L. Goggin and R. J. Goodfellow, *J. Chem. Soc., Dalton Trans.*, 1976, 1959; S. J. Anderson and R. J. Goodfellow, *J. Chem. Soc., Dalton Trans.*, 1977, 1683; H. Motschi, S. N. Sze and P. S. Pregosin, *Helv. Chim. Acta*, 1979, **62**, 2086; J. Browning, P. L. Goggin and R. J. Goodfellow, *J. Chem. Res. (S)*, 1978, 328.
- 20 F. H. Allen, O. Kennard, D. G. Watson, L. Brammer, A. G. Orpen and R. Taylor, *J. Chem. Soc., Perkin Trans. 2*, 1987, S1; A. G. Orpen, L. Brammer, F. H. Allen, O. Kennard, D. G. Watson and R. Taylor, *J. Chem. Soc., Dalton Trans.*, 1989, S1.
- 21 J. Kritzenberger, H. Yersin, K.-J. Range and M. Zabel, *Z. Naturforsch., Teil B*, 1994, **49**, 297.
- 22 K. Fukui, *Theory of Orientation and Stereoselection*, Springer-Verlag, Berlin, 1975.
- 23 D. A. Garnovskii, M. F. C. Guedes da Silva, T. B. Pakhomova, G. Wagner, M. T. Duarte, J. J. R. Fraústo da Silva, A. J. L. Pombeiro and V. Yu. Kukushkin, *Inorg. Chim. Acta*, 2000, **300–302**, 499.
- 24 G. R. Desiraju, *Acc. Chem. Res.*, 1996, **29**, 441.
- 25 V. Yu. Kukushkin, Å. Oskarsson and L. I. Elding, *Inorg. Synth.*, 1997, **31**, 279.
- 26 V. A. Strel'tsov and V. E. Zavodnik, *Kristallografia*, 1989, **34**, 1369.
- 27 G. M. Sheldrick, *SHELXTL User Manual*, Rev. 3, Nicolet XRD Corp., Madison, WI, 1981.
- 28 G. M. Sheldrick, SHELXL 97, University of Göttingen, 1997.
- 29 L. G. Axelrud, Yu. N. Grin, P. Yu. Zavalii, V. K. Pecharsky and V. S. Fundamensky, CSD-universal program package for single crystal and/or powder structure data treatment, *Collected Abstracts, XIIth European Crystallographic Meeting, Moscow*, August 1989, USSR Academy of Sciences, Moscow, 1989, p. 155.
- 30 *International Tables for X-Ray Crystallography*, Kynoch Press, Birmingham, 1974, vol. IV.
- 31 M. W. Schmidt, K. K. Baldrige, J. A. Boatz, S. T. Elbert, M. S. Gordon, J. H. Jensen, S. Koseki, N. Matsunaga, K. A. Nguyen, S. J. Su, T. L. Windus, M. Dupuis and J. A. Montgomery, *J. Comput. Chem.*, 1993, **14**, 1347.
- 32 D. Andrae, U. Haeussermann, M. Dolg, H. Stoll and H. Preuss, *Theor. Chim. Acta*, 1990, **77**, 123.
- 33 R. Ditchfield, W. J. Hehre and J. A. Pople, *J. Chem. Phys.*, 1971, **54**, 724; W. J. Hehre, R. Ditchfield and J. A. Pople, *J. Chem. Phys.*, 1972, **56**, 2257.
- 34 M. M. Francl, W. J. Pietro, W. J. Hehre, J. S. Binkley, M. S. Gordon, D. J. DeFrees and J. A. Pople, *J. Chem. Phys.*, 1982, **77**, 3654.
- 35 P. C. Hariharan and J. A. Pople, *Theor. Chim. Acta*, 1973, **28**, 213.
- 36 J. S. Binkley, J. A. Pople and W. J. Hehre, *J. Am. Chem. Soc.*, 1980, **102**, 939; M. S. Gordon, J. S. Binkley, J. A. Pople, W. J. Pietro and W. J. Hehre, *J. Am. Chem. Soc.*, 1982, **104**, 2797.
- 37 T. H. Dunning, Jr. and P. J. Hay, in *Methods of Electronic Structure Theory*, ed. H. F. Shafer III, Plenum Press, New York, 1977, ch. 1, pp. 1–27.
- 38 T. H. Dunning, *J. Chem. Phys.*, 1971, **55**, 716.
- 39 C. Möller and M. S. Plesset, *Phys. Rev.*, 1934, **46**, 618; J. S. Binkley and J. A. Pople, *Int. J. Quantum Chem.*, 1975, **9**, 229.
- 40 K. Fukui, *Acc. Chem. Res.*, 1981, **14**, 363; C. Gonzalez and H. B. Schlegel, *J. Chem. Phys.*, 1991, **95**, 5853.
- 41 J. G. Kirkwood, *J. Chem. Phys.*, 1934, **2**, 351; L. Onsager, *J. Am. Chem. Soc.*, 1936, **58**, 1486.